

## MATERIAL AND ELECTROCHEMICAL CHARACTERIZATION OF ANCIENT INDIAN OCP PERIOD COPPER

T. LAHA<sup>^</sup>, J. SHANKAR<sup>^</sup>, R. BALASUBRAMANIAM<sup>^\*</sup>, A. TEWARI<sup>^</sup>,  
V.N. PRABHAKAR<sup>^</sup>, D.V. SHARMA<sup>^</sup> AND D. BANERJEE<sup>^</sup>

*(Received 17 May 2002)*

The microstructural and electrochemical characterization of the material of construction (Cu) of an ancient Indian ochre colored pottery (OCP) period (2650 BC-800 BC) anthropomorphic figure has been addressed. The microstructures were analyzed, to obtain the volume fraction of second phase particles and grain sizes in two different sections, by stereological methods. The volume fraction of the second phase inclusions and the grain size were similar in both the sections, thereby indicating that the object was manufactured by casting. The electrochemical behaviour of OCP Cu was characterized and compared with a modern Cu sample by potentiodynamic polarization studies in 3.5% NaCl solution. The corrosion rates in the same solution were determined by Tafel extrapolation technique. While the potentiodynamic polarization behaviour of OCP Cu was similar to that of modern Cu, the corrosion rate of OCP Cu was higher than modern Cu. This has been attributed to the presence of second phase inclusions in OCP Cu.

**Key words :** Anthropomorphic figure; Copper; Electrochemical characterization, Microstructural characterization ; OCP period.

### INTRODUCTION

The recent discovery of 31 anthropomorphic copper figures in 2000 AD from an agricultural field near Madarpur village, Thakurdvara tehsil, Moradabad district in Uttar Pradesh has assumed considerable significance

---

<sup>^</sup>Department of Materials and Metallurgical Engineering, Indian Institute of Technology, Kanpur 208 016, INDIA.

<sup>^</sup>Archaeological Survey of India, Agra Circle, Mall Road, Agra 282 001, INDIA.

<sup>^</sup>Author for correspondence

because it has provided scope for study of ochre colored pottery (OCP) period (2650 BC-800 BC) and copper hoards afresh<sup>1</sup>. Only fourteen copper anthropomorphic figures, of which two were mere fragments, were earlier known to the scholarly world before this discovery. Earlier studies conducted on a sample sectioned from a broken arm of one of the anthropomorphic figures indicated the following<sup>1</sup>. The green surface patina was analyzed by X-ray diffraction as a mixture composed mainly of cuprite and minor amounts of malachite and brochantite. The copper possessed a highly heterogeneous grain structure consisting of equiaxed grains and entrapped second phase particles of spherical shape. The identification of equiaxed grains with straight annealing twins, coring and the spherical shape of the inclusions indicated that the anthropomorphic figures had been cast to shape without any further working operation. The relatively low microhardness (65 to 80 kg/mm<sup>2</sup>) of the sample further confirmed that the sample was a cast structure. Local compositions from several different locations in the metallic matrix and the entrapped inclusions were obtained using an electron probe microanalyzer. The composition of the metal was almost pure Cu, with minor impurities of C and Sb. The major elements identified in the second phase particles were Cu, Pb and S, which indicated that these particles were sulphides. The presence of these sulphides has been discussed in with respect to the Cu extraction process. The present study was undertaken to further understand the microstructural features by image analysis and compare the electrochemical nature of the ancient Cu sample with a modern pure Cu sample. As pure copper is the material of construction of containers to be used for long-term (> 10000 years) storage of nuclear wastes in several countries, it is important to understand the effect of long-term exposure on the corrosion behaviour of Cu.

Stereology, the knowledge of space, is a body of mathematical methods relating three-dimensional parameters, defining the structure, to two-dimensional measurements<sup>3</sup>. Stereological methods provide several useful parameters of the structure from incomplete information, obtained from sections of a lower dimension than the original structure. Quantitative stereology is very efficient for measuring familiar geometric quantities. The parameters, which are relevant to be understood in the case of ancient OCP

copper, are volume fraction of second phase inclusions and the grain size. The procedure for obtaining these parameters are briefly discussed below.

The three main methods to measure Volume fraction ( $\bar{V}_v$ ) are by measurements of areas (areal analysis), lineal intercepts (lineal analysis), and counting of points (point counting)<sup>4</sup>. The area fraction ( $\bar{A}_A$ ) of a phase can be determined by measuring and summing the areas of intersection of that phase in microscopic sections. The linear fractions ( $\bar{L}_L$ ) are obtained from random traverses made on randomly selected plans of polish. The traverses are placed randomly in the three-dimensional structure, and the lineal fraction gives a direct estimate of volume fraction. However, a lineal analysis performed on a single plane of polish can never be more reliable, no matter how many traverses are made, than an areal analysis of the same plane. In the point counting method, the volume fraction can be measured by superimposing a two-dimensional lattice on the structure and estimating the point fraction ( $\bar{P}_p$ ). In the nomenclature of quantitative metallography, the relationship between these parameters is expressed by<sup>4,6</sup>

$$\bar{V}_V = \bar{A}_A = \bar{L}_L = \bar{P}_P. \quad (1)$$

In the case of an aggregate containing grains, cells, or particles, the average distance across these randomly oriented volume elements is the important quantity, rather than a maximum dimension. Such an average distance is called the mean intercept length ( $\bar{L}_3$ ) of those space-filling volume elements. The  $\bar{L}_3$  is defined for a single particle as<sup>4</sup>

$$\bar{L}_3 = \frac{1}{N} \sum (L_3)_i \quad (2)$$

where the subscript 3 refers to the dimensionality of the particle, and the  $(L_3)_i$  are the intercepted lengths from N random penetrations of the particle by a straight test line. This definition allows for the possibility of a particle being intercepted more than once by a single penetration of the test line, thereby rendering the above equation applicable to concave as well as convex bodies.

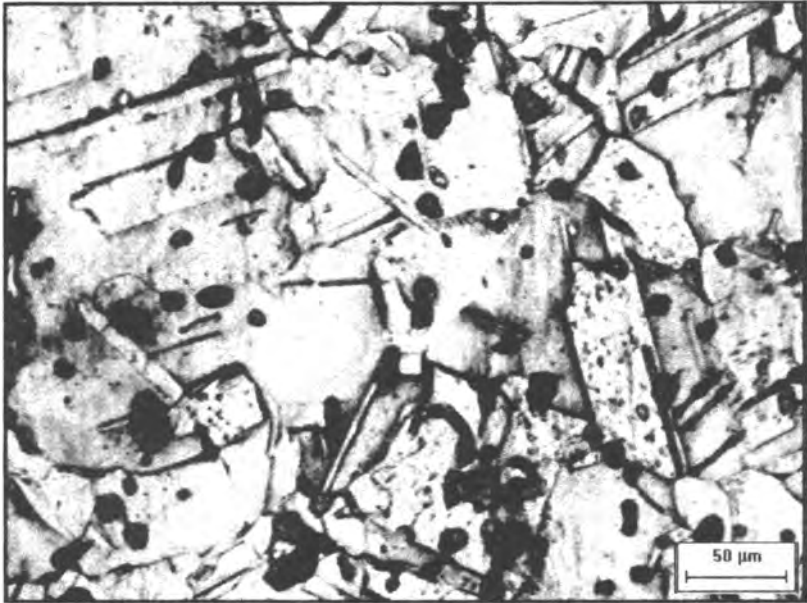
The measurements obtained by stereological methods are statistical in nature and are affected by sampling error. In this regard, the fundamental central-limit theorem is a very powerful tool in statistical analysis in that it provides complete knowledge about the distribution of a random sample from any population. According to this theorem, the standard error of the mean is defined as :

$$\sigma_{\bar{x}} = \frac{\sigma_x}{\sqrt{n}} = \left[ \frac{\sum(x - \bar{x})^2}{n(n-1)} \right]^{1/2} \quad \dots(3)$$

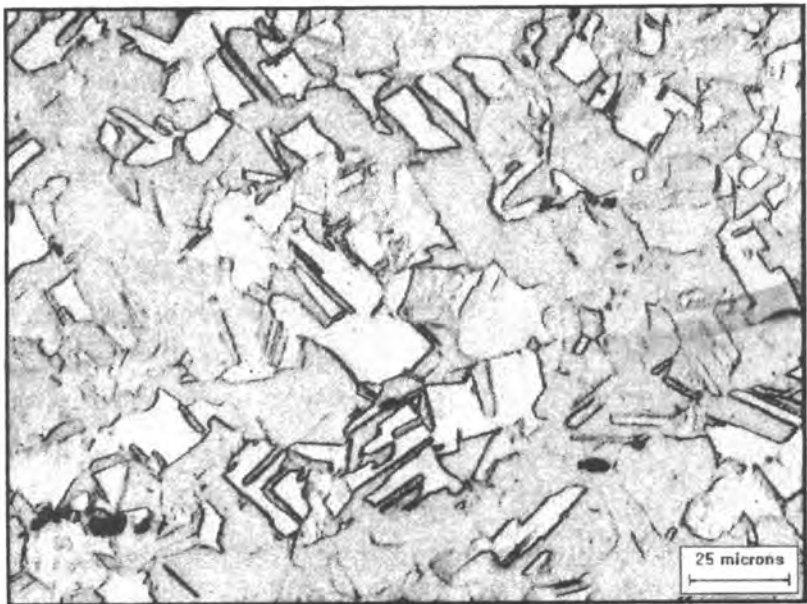
where  $x$  is some random variable,  $\bar{x}$  is the mean of  $x$  for  $n$  number of readings and  $\sigma_x$  is the standard deviation of  $x$ .

#### EXPERIMENTAL PROCEDURE

A broken arm of one of the figures was utilized for the analysis. A small portion of material was sectioned and two sections were prepared for metallographic analysis, one parallel to the surface and another perpendicular to the surface. These specimens have been labelled 'a' and 'b'. A sample of modern pure Cu, sectioned from a plate, was also utilized in the study for reference purpose. All the specimens were hot mounted. Special care was taken during mounting to maintain the flatness of the sample and the mount. The samples were ground carefully to avoid the reappearance of new scratches. The final polishing was performed with 1 $\mu$ m diamond powder. The specimens were etched in ferric chloride solution for revealing the microstructures. The microstructures were recorded using an optical microscope (Axiolab A, Zeiss, Germany), attached with a digital camera (CE, Japan). They were later analyzed by an image-analysis program (Image-Pro Plus 4.1, Media Cybernetics, USA). Microstructural analysis of the OCP Cu revealed second phase inclusions, which appeared dark in the optical micrograph (Fig. 1a). These inclusions were earlier analyzed in an electron probe microanalyzer as sulphides<sup>2</sup> of Cu and Pb. Annealing twins were also observed in several grains. In case of pure Cu, second phase inclusions were not observed (Fig. 1b).



(a)



(b)

Fig. 1 : Optical micrograph of (a) OCP Cu and (b) modern Cu.

The volume fraction of the inclusions and the grain sizes were estimated. In order to measure the volume fraction, 60 fields of view (FOV) were captured (at a magnification of 200X) and analyzed. A  $8 \times 8$  grid was imposed on each of the FOVs. The number of points falling in the feature of interest was calculated manually and divided by the total number of grid points to provide the volume fraction (Eqn 1). The linear intercept method was used for measuring the grain size. Thirty FOVs were captured and five test lines were imposed on each of the FOVs using the software. The number of intersections between the test lines and the grain boundaries were counted. The total length of test lines divided by the total number of intersection points provided the grain size, as per Eqn (2). In order to minimize the statistical error, a higher number of FOVs were analyzed for volume fraction measurements.

One of the OCP Cu samples that was used for the microstructural study (sample *a*) was removed from the mount and re-mounted in a cold setting epoxy, after soldering a conductive wire to it. Electrochemical polarization experiments were conducted utilizing a potentiostat (263A Perkin Elmer, USA). Polarization studies were carried out in 3.50 weight percent NaCl solution. The samples were polished to 4/0 grade emery paper finish. The surface of the samples was cleaned using distilled water and acetone before starting the experiments. A flat cell was used with platinum as the counter electrode and Ag/AgCl in saturated KCl (SSC) (198 mV vs SHE) as the reference electrode. Potentiodynamic polarization experiments were performed to compare the electrochemical behaviour of the samples. Corrosion rates were determined by the Tafel extrapolation procedure. A scan rate of 1 mV/s was used for potentiodynamic polarization experiments and 0.166 mV/s for Tafel extrapolation, as per ASTM standards<sup>7</sup>.

## RESULTS AND DISCUSSION

The results of the microstructural analysis are tabulated in Table 1. The volume fraction of second phase inclusions was almost similar in both the OCP Cu sections. The grain size of the OCP Cu from both the sections was also comparable, therefore attesting to the casting method of production of the anthropomorphic figure.

**Table 1 :** Volume fraction of inclusions and grain size

Sample	Volume fraction			Grain size		
	% $V_v$	Std Dev	% error ( $\pm$ )	Size ( $\mu\text{m}$ )	Std Dev	% error ( $\pm$ )
Modern Cu	-	-	-	19.47	1.57	2.95
OCP Cu (a)	3.99	0.82	5.29	20.47	3.37	6.01
OCP Cu (b)	2.11	0.90	11.02	19.50	3.79	7.09

The potentiodynamic polarization curve in 3.50 wt. % NaCl solution for modern and OCP Cu samples are shown in Fig. 2. Both the copper samples exhibited similar electrochemical behavior in the NaCl solution.

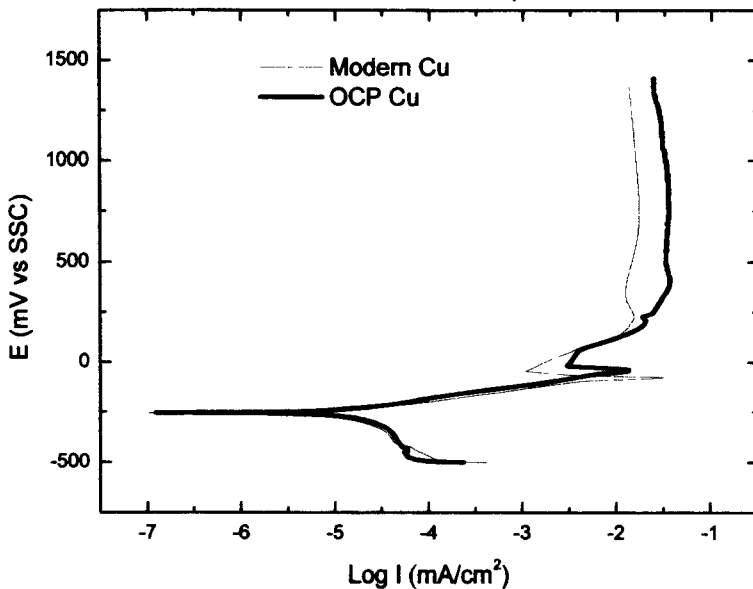


Fig. 2 : Potentiodynamic polarization curves for OCP Cu and modern Cu in 3.50 wt. % NaCl solution.

The polarization behaviour of modern Cu was in excellent agreement with published data<sup>8</sup>. The surface film that formed at anodic potentials was very stable because no pitting was observed even up to + 1400 mV vs SSC. This thin adherent surface film was visually observable in both the samples even after removal from the solution at the end of each experiment. The various potentials like zero current potential, primary passivation potential, etc. are almost similar for both the samples indicating that the samples were thermodynamically similar to each other.

The major difference between the two samples was the presence of second phase inclusions in the case of the OCP Cu sample. The presence of second phase inclusions, however, affected the corrosion rates. The corrosion rates in mils per year (mpy) were estimated from the dissolution rate given by current density using the relation,

$$\text{Corrosion rate} = i (1/\rho) (\Delta)\epsilon$$

where  $\rho$  is the density,  $\Delta$  is a constant of value  $1.2866 \times 10^5$ ,  $\epsilon$  is the equivalent weight and  $i$  is the current density in  $\text{A}/\text{cm}^2$ . The Tafel extrapolation experiment revealed that the corrosion rate of OCP Cu sample (7.3 mpy) was marginally higher than modern Cu (2.2 mpy). The corrosion rate for modern Cu agreed well with the published corrosion rate for Cu in seawater (1-5 mpy)<sup>9</sup>. Similarly, the corrosion rate for OCP Cu was higher than modern Cu in the highly anodic region of the potentiodynamic polarization diagram (Fig. 2), where the current density was nearly constant with increasing potential. The dissolution rate for OCP Cu was  $36.3 \text{ mA}/\text{cm}^2$  ( $= 11047 \text{ mpy}$ ) while that for modern Cu was  $17.0 \text{ mA}/\text{cm}^2$  ( $= 5185 \text{ mpy}$ ). The major effect of second phase slag particles was to enhance the dissolution tendencies. This probably resulted due to galvanic coupling action of the Cu matrix with the slag inclusions.

### CONCLUSIONS

The microstructure of the material of construction of an OCP period (2650 BC-800 BC) copper object has been characterized by stereological methods. The volume fraction of second phase particles and the grain sizes were estimated in two sections. The similar magnitude of volume fraction and the grain size in both the sections confirmed that the object was manufactured by casting without any further thermomechanical processing. The electrochemical behaviour of OCP Cu has been characterized and compared with a modern Cu sample by potentiodynamic polarization studies and the corrosion rates were determined by Tafel extrapolation technique in 3.5% NaCl solution. The polarization behaviour of OCP Cu was similar to that of modern Cu; however, the corrosion rate of OCP Cu was higher than modern Cu. The



higher rates of corrosion in case of OCP Cu has been attributed to the presence of second phase inclusions.

### NOTES AND REFERENCES

1. R. Balasubramaniam, M.N. Mungole, V.N. Prabhakar, D.V. Sharma and D. Banerjee, "Studies on Ancient Indian OCP Copper", *IJHS*, 37.1 (2002) 1-15.
2. B. Rosborg, O. Karnland, G. Quirk and L. Werme, "Measurements of Copper Corrosion in the LOT Project at the Aspo Hard Rock Laboratory", *Proceedings of the International Workshop on Prediction of Long Term Corrosion Behaviour in Nuclear Waste Systems*, European Federation of Corrosion, Series 42, 2002 (in press).
3. E.R. Weibel, *Stereological Methods*, Vol. 2, Academic Press, New York, 1980, pp. 1-18.
4. E.E. Underwood, *Quantitative Stereology*, Addition-Wesley, New York, 1970, pp. 25-82.
5. H. Fischmeister, *Computers in Material Technology*, ed. T. Ericsson, Pergamon Press, London, 1980, pp. 109-129.
6. J.E. Hilliard, *Quantitative Microscopy*, ed. R.T. Dehoff and F.N. Rhines, McGraw-Hill Book Company, New York, 1968, pp. 45-76.
7. *Metals Test Methods and Analytical Procedures*, Annual Book of ASTM Standards, Volume 3.02, Section 3, Philadelphia, USA, 1987.
8. K.R. Trethewey and J. Chamberlain, *Corrosion for Students of Science and Engineering*, Longman Scientific, Harlow, 1988, p. 92.
9. F.L. LaQue, *Marine Corrosion-Causes and Prevention*, John Wiley, New York, 1975, p. 146.